Density fluctuation phenomena in the scrape-off layer and edge plasma of the Wendelstein 7-AS stellarator

S. Zoletnik
KFKI-Research Institute for Particle and Nuclear Physics, P.O. Box 49, H-1525 Budapest, Hungary

M. Anton, M. Endler, S. Fiedler, M. Hirsch, K. McCormick, J. Schweinzer, and the W7-AS Team
Max-Planck Institut für Plasmaphysik, Association Euratom, Boltzmannstrasse 2, D-85748 Garching bei München, Germany

(Received 16 November 1998; accepted 26 July 1999)

The fluctuation of electron density in the scrape-off layer (SOL) and edge plasma regions of the Wendelstein 7-AS stellarator [H. Renner *et al.*, Plasma Phys Controlled Fusion **31**, 1579 (1989)] is investigated by the beam emission spectroscopy technique, observing fluctuations in the Li($2p$) line emission intensity of a 50 keV accelerated Li beam. A recently developed numerical technique enables correct reconstruction of correlation functions (and as a consequence, fluctuation amplitudes as well) of the electron density fluctuations from correlations of beam light fluctuations. Depending on the plasma electron density, the radial range of the measurement is either limited to $r/a>0.9$ (at the highest densities) or can extend to about $r/a>0.3$ at the lowest densities. As the technique is nonperturbing to the plasma, several hundred shots were analyzed and a catalog of the observed phenomena was established. The results always show a change in the properties of the fluctuations at approximately the last closed flux surface. This observation might indicate differences in the turbulence drive in the SOL and the edge plasma. However, one cannot exclude that the same turbulence phenomenon results in different density fluctuations in the two regions due to the different magnetic topologies. The relevance of the observed phenomena to anomalous transport is discussed. © *1999 American Institute of Physics.* [S1070-664X(99)00711-9]

I. INTRODUCTION

Turbulence in magnetically confined fusion plasmas is considered to be one of the key issues for the understanding of transport across the confining magnetic field.[1,2] As turbulence should cause fluctuations in the plasma parameters (density, temperature, etc.), measurement of these fluctuations is thought to deliver information on the underlying physical processes. However, measuring only the amplitude of the fluctuations proved to be inadequate, as the fluctuation amplitude itself does not always correlate with changes in confinement quality.[2] To get reasonable insight into the processes, one needs a spatially and temporally well-resolved measurement of several plasma parameters and their cross correlations. Up to now, such measurements could be performed in the scrape-off layer (SOL) and in the edge plasma on small devices, where the relatively tenuous and cold plasma enables the insertion of material probes. Measurements with Langmuir probes revealed that electrostatic fluctuations, although with high uncertainty, can account for both the particle and heat transport.[1]

The spatial and temporal structure of the SOL turbulence were analyzed in great detail for both tokamaks[3,4] and stellarators[5] and the properties were found to be rather similar in all cases, showing several 10% rms relative fluctuation amplitudes, centimeter scale random structures both poloidally and radially, with several meters toroidal correlation length and some 10 μs lifetime. Some sign of periodicity is often observed in the poloidal direction. These structures are seen to propagate poloidally in the ion diamagnetic drift direction.

In the confinement region data are less detailed, but two-point correlation measurements of density fluctuations with a heavy ion beam (HIBP) diagnostic[6] and reflectometry[7] and multipoint measurements with beam emission spectroscopy (BES)[8] showed correlation lengths in the few centimeter range in both the poloidal and radial directions. The fluctuation amplitudes do not exceed a few percent relative to the average density, and lifetimes are in the few microsecond range. Electron temperature fluctuations with similar characteristics were also detected.[9]

Despite the general finding that centimeter scale poloidal and radial structures are present in the turbulence, experiments pointed out both strong poloidal asymmetries[10] and radial dependencies,[6] even in the confinement region. Of special importance is the region around the last closed flux surface (LCFS), where the relative fluctuation levels change by an order of magnitude within a few centimeters and where changes in turbulence are thought to be responsible for the L–H (low to high) mode transition. Turbulence around the LCFS was extensively investigated at the Advanced Toroidal Facility (ATF)[11,12] and it was concluded that the drive is likely to be different in the SOL and the confinement region.

Provided the finding that centimeter scale structures may play an important role in turbulence the accelerated Li-beam diagnostic[13] at Wendelstein 7-AS (W7-AS),[14] having a beam diameter of about 1.5 cm was found to be extremely suitable

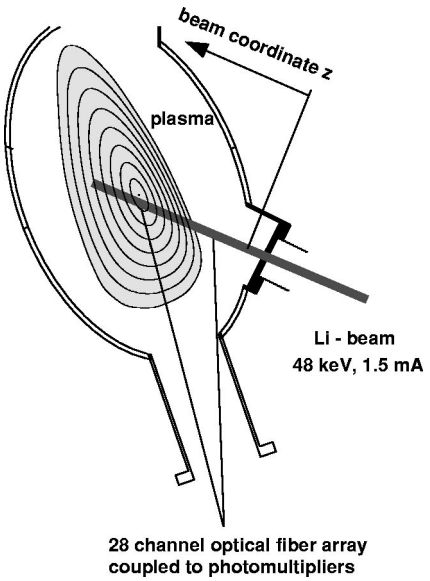

FIG. 1. The Li-beam diagnostic at W7-AS (schematic).

for electron density fluctuation measurements. Depending on the plasma electron density, the radial range of this diagnostic is either limited to $r/a>0.9$ (at the highest densities) or can extend to about $r/a>0.3$ at the lowest densities, thus, in any case, a few centimeters of the edge plasma layer can be measured. Recently a new technique[15] has been developed which enables the correct determination of spatiotemporal correlation functions of electron density fluctuations from the measured correlation functions of beam light fluctuations. As the beam represents a nonperturbing diagnostic, data were taken and analyzed for a large number of shots under widely different plasma parameters and heating scenarios. To complement the poloidally localized but radially resolved BES measurement, magnetic field fluctuations were recorded and correlated with Li-light fluctuations using poloidal arrays of Mirnov coils mounted on the vessel wall at three toroidal positions.

This paper characterizes fluctuation phenomena seen in the experiment and addresses the question whether density fluctuations observed in the SOL and in the first few centimeter of the confinement region are identical.

II. EXPERIMENT AND DATA EVALUATION

The 50 keV Li beam penetrates the W7-AS plasma in an elliptic cross-section traveling nearly across the magnetic axis, as is shown in Fig. 1. The Li($2p$) line radiation induced by collisions of plasma particles with neutral Li-beam atoms is collected by an optic equipped with an interference filter and imaged onto a set of 28 light guides. Each light guide is coupled to a separate photomultiplier. The spatial resolution of the setup in the SOL is approximately 0.5 cm, while at the end of the observation line it is about 1 cm. The photomultiplier signal amplifiers have a bandwidth of more than 1 MHz. Each of the 28 signals is measured in two analog-to-digital converter (ADC) channels. One channel samples the signal after appropriate low-pass filtering at a sampling rate of 5 kHz over the full discharge time and additionally over some calibration time after it. Another separate ADC samples at a rate between 200 kHz and 1 MHz, but only over a few hundred milliseconds. The low frequency part of the signal is used for determining the electron density profile from the Li($2p$) light signals[16] and also for relative calibration of the 28 channels in a gas pulse following the plasma discharge. The high frequency component is used for the fluctuation measurement taking calibration factors from the low frequency signals. It should be noted, that no *absolute* calibration of the channels is necessary, the absolute electron density profile is reconstructed from the *relative* light profile. The electron temperature profile and the Z_{eff} profile are also required as input parameters for the density calculation program. The electron temperature was taken from Thomson scattering, while $Z_{\mathrm{eff}}=2$ was assumed over the whole plasma. The accuracy of these parameters does not effect the density calculation significantly.

The light detected by the photomultipliers consists not only of the Li($2p$) light of the beam, but may contain a considerable amount of continuum and other line radiation from the plasma as well. To check the intensity of this background light, the beam was chopped in regular intervals during the discharge by deflecting it in the Li gun before neutralization. The signal detected during beam-off times is referred to as background signal.

Photon statistical noise on the low frequency signals is not more than 1%, thus density profiles can be reconstructed even for a single measured time point. In the high frequency channels photon statistical noise does not decrease below 10% even at the maximum of the light profile. This fact makes the reconstruction of density profiles from single time point measurements impossible. However, correlation functions

$$C^S(Z_1,Z_2,\tau)=\frac{1}{T}\int_0^T \tilde{S}(Z_1,t)\tilde{S}(Z_2,t+\tau)dt \qquad (1)$$

can be determined with good accuracy if the integration time T is set long enough. Here $\tilde{S}(Z,t)$ denotes the fluctuating part of the light emission detected at point Z along the beam as a function of time. The light signal is not only a function of the local plasma parameters, but contains the effect of the whole plasma layer along the beam from the vessel wall to Z. Two effects cause this nonlocality. One is the finite relaxational time of the atomic processes in the beam, which in conjunction with the beam velocity causes an approximately 3 cm smoothing of the light profile relative to the density profile. The other effect is ionization, as ionized atoms leave the beam, and in response to a local density increase at Z_0, the light signal decreases for $Z>Z_0$. In low density discharges and especially in the SOL ionization is negligible and, thus, for structures having several centimeter radial correlation length, the Li-beam light signal is nearly proportional to the electron density.

Reference 15 describes a method for obtaining the correlation functions of electron density fluctuations from the measured correlation functions of beam light fluctuations. Here we present an overview of the technique, so please refer to the original publication[15] for details. Using an appro-

priate model of the atomic processes taking place in the beam,[16] the light emission $S(Z)$ for any density profile $n_e(Z)$ can be calculated:

$$S(Z)=\mathcal{F}\{n_e(Z)\}. \tag{2}$$

We write both the beam light and electron density as a sum of a time independent and a fluctuating part,

$$S(Z)=S^0(Z)+\tilde{S}(Z,t), \quad n_e(Z)=n_e^0(Z)+\tilde{n}_e(Z,t). \tag{3}$$

If the beam is only weakly attenuated or the electron density fluctuation amplitude is small ($\leqslant 10\%$) then the connection between the beam light fluctuations and the electron density fluctuations can be approximated linearly but nonlocally:

$$\tilde{S}(Z,t)\approx\int_0^Z \tilde{n}_e(Z',t)h(Z,Z')dZ', \tag{4}$$

where $h(Z,Z')$ describes the effect of a small density change at Z' on the light emission at Z. Weak attenuation holds for the SOL, while the condition of low fluctuation level is satisfied for the confinement region. Therefore, the above linearization is a good approximation everywhere along the Li beam for nearly all discharge conditions. For certain density and fluctuation amplitude profiles linearity was tested.

The $h(Z,Z')$ function depends on the mean electron density profile and other plasma parameters. It is determined numerically by calculating the change in light profile at Z in response to a small amplitude density peak $\delta n\Delta_{Z'}(Z)$ added to the main density profile around Z':

$$h(Z,Z')=\frac{\mathcal{F}\{n_e(Z)+\delta n\Delta_{Z'}(Z)\}-\mathcal{F}\{n_e(Z)\}}{\delta n}. \tag{5}$$

$\Delta_{Z'}(Z)=1$ at $Z=Z'$ and linearly goes to zero in a finite length. δn is selected as small, so as to be surely well below the linearity limit. By substituting the linear approximation of Eq. (4) into Eq. (1), one arrives at a linear mapping from the correlation functions of the electron density fluctuations to the correlation functions of beam light fluctuations:

$$C^S(Z_1,Z_2,\tau)=\int_0^{Z_1}\int_0^{Z_2}h(Z_1,Z')h(Z_2,Z'')C^n(Z',Z'',\tau)dZ'\,dZ'', \tag{6}$$

where $C^n(Z_1,Z_2,\tau)$ is the cross-correlation function of electron density fluctuations defined similarly to Eq. (1) as

$$C^n(Z_1,Z_2,\tau)=\frac{1}{T}\int_0^T \tilde{n}_e(Z_1,t)\tilde{n}_e(Z_2,t+\tau)dt. \tag{7}$$

By inverting Eq. (6) as described in detail in Ref. 15 one can calculate the correlation functions of electron density fluctuations. It has to be emphasized that this inversion yields the correlation function of electron density fluctuations in *absolute* units although the beam light profile is only *relatively* calibrated. This feature is made possible by the density calculation program[16] which calculates the electron density profile in *absolute* units from the *relatively* calibrated light profile, and thus establishes the necessary scaling factor for transformation $\mathcal{F}$.

The rms fluctuation amplitude is calculated from the cross-correlation functions:

$$\sqrt{\langle\tilde{n}_e^2(Z,t)\rangle}=\sqrt{C^n(Z,Z,0)}, \tag{8}$$

where $\langle\cdots\rangle$ means temporal averaging. The usual normalized correlation functions are approximated as

$$\bar{C}(Z_1,Z_2,\tau)=\frac{C(Z_1,Z_2,\tau)}{\sqrt{C(Z_1,Z_1,0)C(Z_2,Z_2,0)}}, \tag{9}$$

both for the beam light and for the electron density.

In the actual calculations the correlation functions of electron density fluctuations are determined at a finite set of points along the beam. Other details of the method, e.g., handling of photon noise, determination of error bars, are described in detail in Ref. 15.

The temporal resolution of the correlation functions (resolution in τ) can be as good as 1 μs, but in order to reduce statistical noise it is typically set to about 5 μs. The temporal resolution in real discharge time is determined by the minimal integration time T needed to determine the correlation functions, and is typically 10 ms. Spatial resolution of the density cross-correlation functions is in most cases set to 1 cm. The minimum detectable fluctuation level depends on the integration time. For 100 ms integration time it can be as low as 1%.

Magnetic field fluctuations are measured by sampling the signals of Mirnov coils with 3–5 μs time resolution. By applying the singular value decomposition (SVD) technique to a poloidally distributed set of Mirnov coils at one toroidal position the dominant spatial and temporal structures are determined.[17] Additionally, the correlation between Mirnov coil signals and Li-beam light signals is calculated. Although this correlation can be different from the correlation between electron density fluctuations and magnetic field fluctuations, it can deliver valuable information. At least for low density discharges the beam light fluctuation correlation functions are close to the correlation functions of electron density fluctuations.

III. EXPERIMENTAL RESULTS

A. Fluctuation amplitude

A large number of discharges under various plasma conditions, edge rotational transform $\iota_a=0.25-0.55$, central electron density $n_e(0)=1-8\times10^{19}\,\mathrm{m}^{-3}$ and heating scenarios including electron cyclotron resonance heating (ECRH), neutral beam injection (NBI), ion cyclotron resonance heating (ICRH) and combined were analyzed with the Li-beam fluctuation diagnostic. Profiles of electron density, Li($2p$) light intensity, and $\tilde{n}_e$ rms amplitude are shown in Fig. 2 for three discharges with different electron densities but otherwise the same conditions. The relative fluctuation levels show the usual tendency observed on W7-AS and other devices as well. Several 10% fluctuation level is seen in the SOL, which drops to 1%–3% a few centimeters inside the LCFS. The absolute magnitude of density fluctuations peaks 1–2 cm inside the LCFS. The relative fluctuation levels show a plateau close to the LCFS.

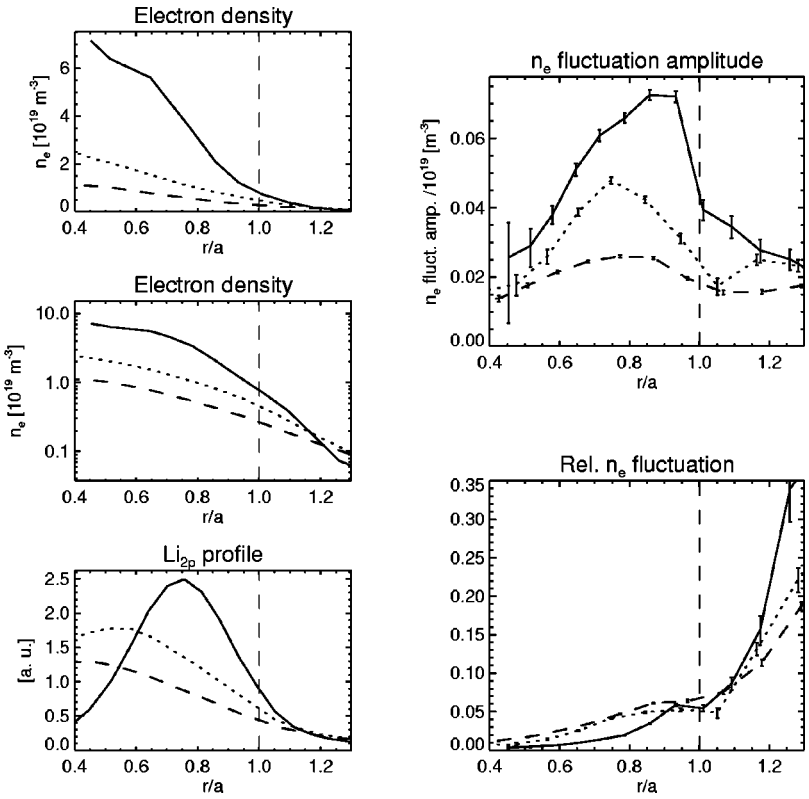

FIG. 2. Profiles of electron density (linear and logarithmic scale), Li($2p$) light, electron density fluctuation amplitude and relative electron density fluctuation amplitude as a function of normalized minor radius. The different curves show discharges with different electron densities. All discharges are at $\iota_a = 0.347$, $B_0 = 2.5\,T$, 140 GHz ECRH heating (400 kW).

The absolute fluctuation amplitude at the LCFS increases with increasing density, but $\tilde{n}_e/n_e$ stays nearly constant at a level of 5%–7%. $\tilde{n}_e$ increases on the inner side of the LCFS as well, but not as much as the main density. As a consequence, in the confinement region $\tilde{n}_e/n_e$ falls off faster for the higher density discharge. In the SOL the trend is reversed, the relative fluctuation level increases with increasing plasma line averaged density. The same observations were made by comparing profiles at different line integrated densities at $B_0 = 1.25\,\mathrm{T}$ and 70 GHz ECRH. It should be noted that, as numerical simulations showed, this behavior is not the result of increasing beam attenuation as a function of line integrated plasma density. The effect of beam attenuation manifests itself rather in the increase of the error bars, as can be seen in Fig. 2.

A substantial deviation from the above fluctuation amplitude profile is observed in NBI heated discharges. In these cases $\tilde{n}_e/n_e$ does not drop to 1% but stays above 5%, while Mirnov coil and x-ray signals show mode activity. The relatively high electron density and the high fluctuation amplitude make the linear approximation of Eq. (4) questionable and the reconstruction of the density fluctuation correlation functions is done only up to the LCFS. This mode activity will be discussed in more detail later.

B. Catalog of fluctuation phenomena

The temporal behavior of density fluctuations was investigated by analyzing the autocorrelation functions $A(Z,\tau) = C(Z,Z,\tau)$ at different Z coordinates along the beam. Figure 3 plots autocorrelation functions at five positions around the LCFS. The temporal behavior of the turbulence at and inside the LCFS is obviously different from the fluctuations in the SOL and suggests that more than one phenomenon is present in the plasma. The fluctuations in the SOL will be referred to as ''SOL turbulence,'' while the fluctuation inside the LCFS will be called ''wave-like,'' referring to the wavepackage-like shape of the autocorrelation function. In addition to these two basic phenomena, other kinds of fluctuations are also observed under different discharge conditions. These different phenomena are characterized as follows.

(1) *SOL turbulence*: Fluctuations with 10%–40% relative amplitude are always present in the SOL. Their autocorrelation functions are monotonically falling with increasing time lag, this way no characteristic frequencies are present in the fluctuation. The autocorrelation time (*e*-folding time of the autocorrelation functions) is between 20 and 50 μs and decreases towards the LCFS. Some slight (<0.2) negative correlation is sometimes observed at around 100 μs time delay, which is probably an indication of the poloidally periodic structure observed in H_α light measurements.[4,5] The radial correlation length is 1–2 cm. These fluctuations are always present in the SOL and their characteristics are not sensitive to edge ι changes. A typical spatiotemporal correlation function of SOL fluctuations is shown in Fig. 4(a). Both inward and outward radial propagation can be observed, depending on the plasma discharge. This fact is most probably a combined effect of the inclination of the structures in the radial-poloidal plane[18] and the poloidal flow velocity. These characteristics are in good agreement with probe measurements in the SOL on W7-AS[5,18,19] and on other machines.[1,4] No correlation was observed between SOL density and magnetic field fluctuations, as is shown in Fig. 5.

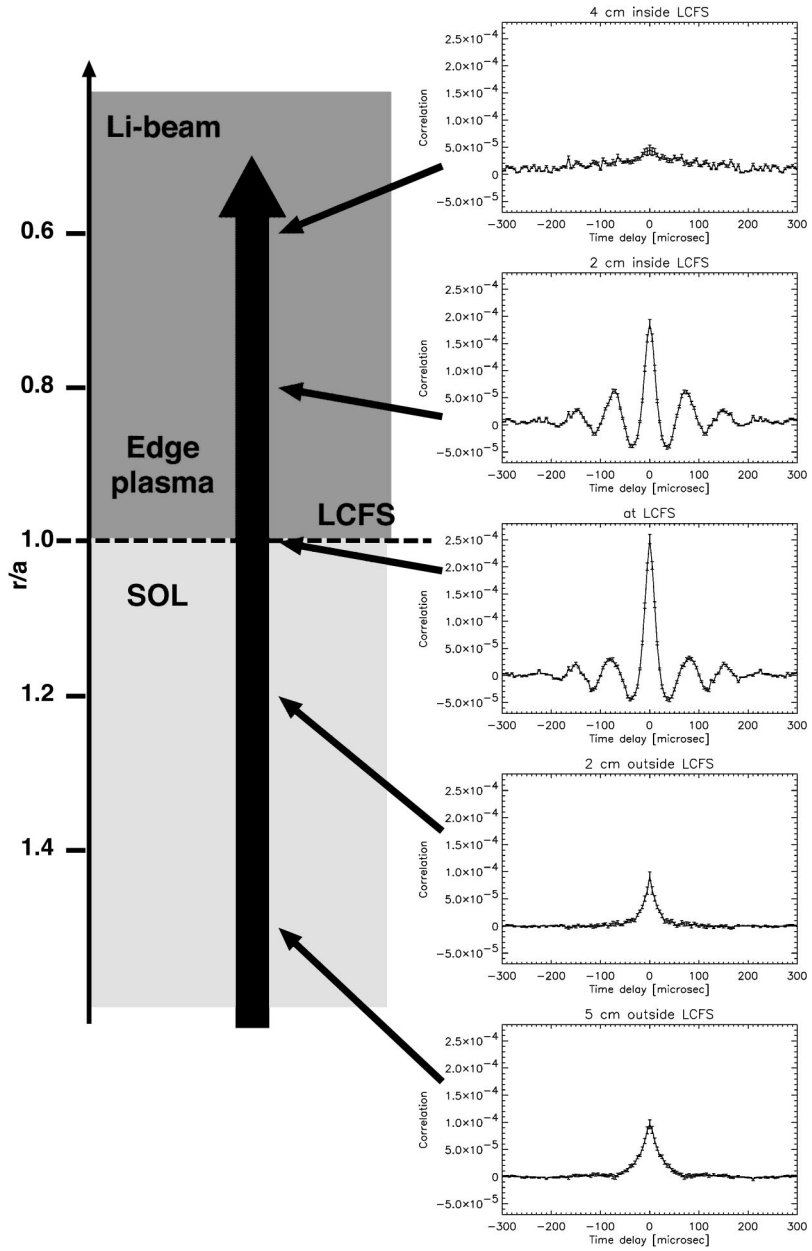

FIG. 3. Autocorrelation functions of electron density fluctuations at different positions along the Li beam for a low density $[n_e(\max)=1\times10^{19}\,\mathrm{m}^{-3}]$ ECRH discharge. The functions are not normalized, thus their amplitude at $\tau=0$ corresponds to $\langle\tilde{n}_e^2\rangle$ in units $[10^{19}\,\mathrm{m}^{-3}]^2$.

(2) *Wave-like fluctuations*: In the edge layer of the confinement region the fluctuations differ from the SOL turbulence, as can be observed in Fig. 3. The autocorrelation functions tend to be wave-like, e.g., they show a few minima and maxima before falling to zero. The number of minima depends on the discharge parameters and changes from 0 to about 5–6, i.e., the periodic nature is not always present. The time delay between maxima is in the 30–100 μs range, thus

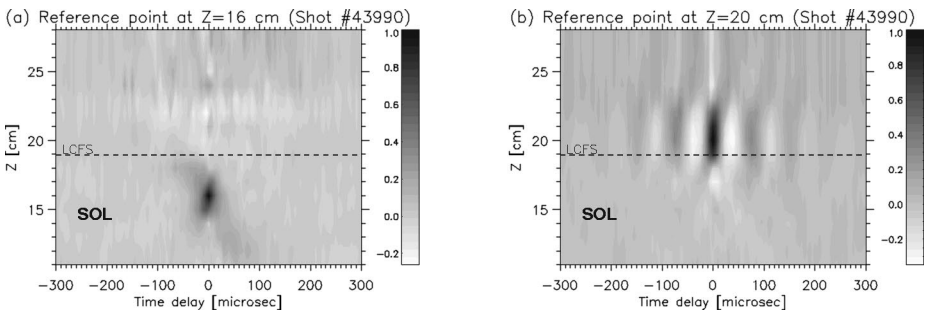

FIG. 4. Normalized spatiotemporal correlation of electron density fluctuations relative to (a) a point in the SOL, (b) a point 1 cm inside the LCFS. The horizontal axis plots time lag, vertical axis is coordinate along the Li beam.

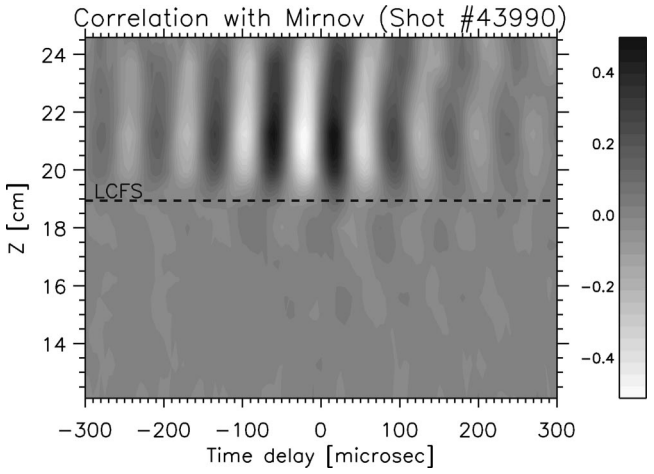

FIG. 5. Normalized correlation of Mirnov coil signal with all Li-beam light signals. The horizontal axis gives time lag, the vertical, distance along the beam.

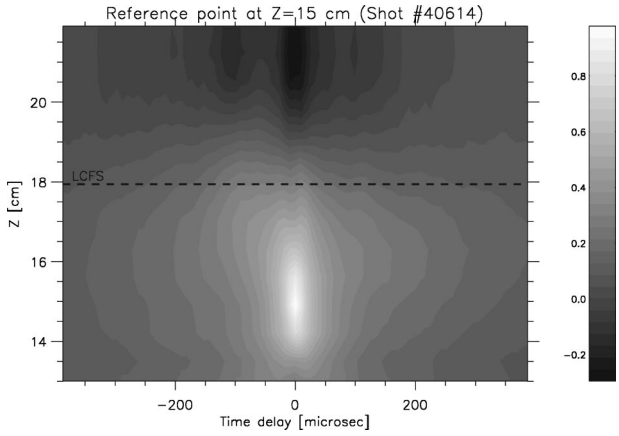

FIG. 6. Normalized spatiotemporal correlation of electron density fluctuations during relaxational phenomena. Reference point is in the SOL. The horizontal axis gives time lag, the vertical, distance along the beam.

the frequency of the oscillations in the wavepackage (f_{wave}) is between 10 and 30 kHz. A typical spatiotemporal correlation function of the wave-like fluctuations is plotted in Fig. 4(b).

These fluctuations are correlated with magnetic field fluctuations (see Fig. 5) measured by Mirnov coils near the vessel wall. Normalized correlations between beam-light and magnetic field fluctuations are between 0.2 and 0.7, depending on plasma parameters. The amplitude of the correlation between Li-beam signals and Mirnov coils located at different positions around the chamber is approximately the same, only the phase depends on the coil location. This correlation enables us to complement the radially resolved but poloidally localized BES density fluctuation measurement with analysis of signals from a poloidal set of Mirnov coils located at a toroidal section of W7-AS. Using SVD analysis[17] the dominant spatial pattern of the magnetic field fluctuations was determined. It was found that the poloidal structure can be best described by a rotating perturbation of poloidal mode number $m=\mathrm{int}(1/\iota_a)$, where int( ) means the closest integer. For example, $m=3$ is observed close to $\iota_a=1/3$, while around $\iota_a=1/2$ the mode number is $m=2$. The wave-like nature of density fluctuations follows from the poloidal rotation of these structures. It has to be noted that both the absolute value and the radial distribution of the phase between the density and magnetic field fluctuations depend strongly on ι.

The layer in which these fluctuations are present extends to a maximum of 30% of the minor radius ($r/a>0.7$), but the extent, and all other parameters, depend sensitively on the magnetic configuration and plasma parameters. The radial correlation length is comparable to the width of the layer in which these fluctuations are seen. Due to about 1 cm uncertainty in the location of the LCFS it is not clear whether wave-like fluctuations appear only inside the LCFS or in the last cm of the SOL as well.

(3) *Relaxational phenomena*: Under certain plasma conditions, density fluctuations with 200–500 μs correlation time appear both in the SOL and the edge plasma. They are most characteristic in a small ι range around $\iota_a=0.523$ where they are the result of edge localized mode (ELM)-like sudden flattenings of the density profile followed by a gradual relaxation around the LCFS.[20–22] These events are correlated with peaks in the edge H_α radiation intensity. In this ι range the fluctuations modulate even the background light so strongly that the reconstruction of $\tilde{n}_e$ correlation functions is impossible. However, outside of this ι range relaxational phenomena are less pronounced and one can calculate the $\tilde{n}_e$ correlations as well. An example is shown in Fig. 6. A flattening of the density profile is reflected in a radial anticorrelation between positions inside and outside the LCFS.

(4) *Mode activity*: In NBI heated discharges one can often observe periodic autocorrelation functions of the Li-beam light fluctuations as plotted in Fig. 7. As the amplitudes are high in the confinement region as well, a correct reconstruction of $\tilde{n}_e$ correlations is not possible inside the LCFS with the present numerical algorithm.

Fluctuations of this kind in the electron density are always accompanied by periodic fluctuations in Mirnov coil signals and soft x-ray emission. The high resolution soft x-ray tomography system on W7-AS identified these fluctuations as poloidally rotating global Alfvén eigenmodes (GAE).[23] Although these fluctuations modulate the plasma

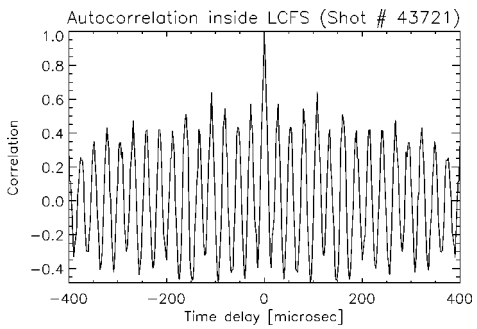

FIG. 7. Normalized autocorrelation of Li-beam light fluctuations 2 cm inside LCFS during GAE mode activity.

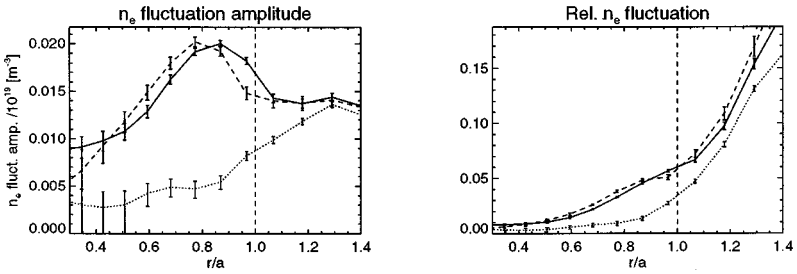

FIG. 8. Change in absolute and relative electron density fluctuation amplitude during a current ramp experiment. Fluctuation amplitudes before current (—), with 2 kA current (···) and after current (- - -). Plasma parameters were $\iota_a=0.347$ (at $I_p=0$), $B_0=2.5$ *T*, $n_e(\max)=1\times10^{19}\,\mathrm{m}^{-3}$, 140 GHz ECRH (400 kW). For further explanation see the text.

density in the confinement region much more than other phenomena described in this paper, they usually have no effect on plasma confinement.

C. Sensitivity to plasma parameters

To demonstrate the different sensitivity of the wave-like and SOL fluctuations to magnetic configuration changes, a low electron density $[n_e(\max)=1\times10^{19}\,\mathrm{m}^{-3}]$ current-ramp experiment is presented in Fig. 8. Normally W7-AS is operated in a net-current free configuration, i.e., the ohmic transformer compensates the total plasma current to zero. In the experiment presented in Fig. 8, the total current was driven linearly in time from 0 to 2 kA in 100 ms, then ramped back to 0 at the same rate. Figure 8 shows the absolute and relative density fluctuation amplitudes before, on top of, and after the current pulse. As can be seen, the fluctuations in the outer SOL do not change significantly with the plasma current, while inside the LCFS they drop to one-fourth of the original value almost to the detection limit of about 1%. The hump in the absolute fluctuation level and the corresponding plateau in the relative fluctuation amplitude profile disappear. At the same time, the correlation between Mirnov-coil signals and the Li-beam signals inside the LCFS disappears, and no ''wave-like'' fluctuations can be seen with the Li-beam diagnostic. The Mirnov coils do not detect the wave-like fluctuations, this way they disappear everywhere in the plasma. After the current ramp the fluctuation level goes nearly back to its original value, demonstrating that the phenomena are reproducible. From this behavior one can conclude that the hump in the absolute fluctuation amplitude profile (and the associated plateau in the relative profile) is produced by the ''wave-like'' fluctuations. Without this phenomenon the density fluctuation amplitude drops continously inside the LCFS.

Repeating the same experiment at twice the electron density, basically the same behavior is observed. However, at a much higher density $[n_e(\max)=8\times10^{19}\,\mathrm{m}^{-3}]$, the fluctuations do not disappear. At present it is not yet clear whether this difference is caused by a difference in ι profile due to the higher plasma β or by some other effect.

It is especially interesting to analyze changes in global plasma confinement during the current ramp experiment when the edge fluctuations clearly change. Surprisingly, for the low density case, the diamagnetically measured stored energy is the same for the $I_p=0$ and $I_p=2$ kA case. On the other hand, in the high density current ramp experiment (when the fluctuation amplitudes do not change significantly around the LCFS) the stored energy at $I_p=2$ kA is only half of its value at $I_p=0$.

IV. DISCUSSION

The experimental results described in Sec. III revealed that the Li-beam BES diagnostic is extremely useful as a nonperturbing density fluctuation measurement, especially for the outer one-third of the plasma minor radius on W7-AS. At low densities the measurement range extends even to the core plasma. Different fluctuation phenomena with different radial ranges and dependencies on plasma parameters are observed. In most cases, several of these phenomena are present at the same time. The basic question is which of these are relevant to transport across magnetic flux surfaces and hence to confinement.

Relaxational phenomena are a result of a sudden density profile flattening in the vicinity of the LCFS, thus they should be connected to transport. Indeed a suppression of these events leads to a moderate improvement in confinement. However, the density profile flattening is most probably a response to the enhanced radial transport due to an instability, which is not visible for the Li-beam diagnostic either due to its short correlation length (<1 cm) or high frequency (>1 MHz).[22]

Mode activity observed by the Li beam is only the effect of global modes on the plasma edge, therefore they are not discussed here.

We shall concentrate on the two remaining phenomena, namely on SOL turbulence and wave-like fluctuations. These are localized on the two opposite sides of the LCFS. Although an overlapping in their radial extension around the LCFS is obvious, their radial ranges are basically separated.

The first question which should be addressed is whether SOL and wave-like fluctuations are really two phenomena or represent two manifestations of the same phenomenon. There are several indications that they are really different.

(1) SOL fluctuations are not correlated with magnetic field fluctuations, while wave-like fluctuations are well correlated. This involves that magnetic field fluctuations measured outside the plasma are correlated only to density fluctuations inside the LCFS. This behavior was observed on Texas Experimental Tokamak (TEXT)[24] and an increase of correlation inside the shear layer was also seen on the Divertor Injection Tokamak Experiment (DITE).[25]

(2) Although the Li-beam diagnostic has no poloidal

resolution, the approximate poloidal wavelength of the fluctuations can be estimated for both the SOL and wave-like fluctuations. As all parameters of the SOL turbulence seen by the Li-beam diagnostic agree with Langmuir probe and H_α measurements, the poloidal wavelength should be the same as measured by the probes,[5] i.e., approximately $\lambda_{SOL} = 5$ cm. On the other hand, the poloidal structure of wave-like fluctuations is determined from the poloidal structure of the correlated magnetic field fluctuations. Dividing the circumference of the LCFS by either 2 or 3 (as Mirnov coil measurements indicate either $m=2$ or $m=3$, depending on edge ι) one gets $\lambda_{wave}=30-50$ cm wavelength, nearly an order of magnitude longer than for the SOL turbulence. On the other hand, if the wave-like fluctuations had a local 5 cm wavelength structure in addition to the global low-m one, the Li-beam diagnostic would measure an oscillation with a frequency $f=(\lambda_{wave}/\lambda_{SOL})f_{wave}$ within each of the peaks in the autocorrelation functions. After substituting the wavelengths and f_{wave} into the above expression, f turns out to be between 100 and 300 kHz, which would be easily detectable but was never seen.

(3) As was shown in Sec. III C, the wave-like fluctuations disappear under certain magnetic configurations, while the SOL turbulence does not change significantly.

The above arguments indicate that the density fluctuations on the SOL and confinement zone side of the LCFS are different, as has also been found on ATF.[11,12] However, due to an uncertainty of the LCFS position and the 1 cm radial resolution of the Li-beam density fluctuation diagnostic it cannot be ruled out, that at approximately 1 cm length, the SOL fluctuations are still present in the confinement region and that wave-like fluctuations extend into the edge of the SOL.

Relevance of SOL and wave-like fluctuation to transport: As is known from the literature[2] the energy confinement time in both tokamaks and stellarators increases as a function of average density until a saturation sets in. It was also shown that relative density fluctuation amplitudes at the edge decrease at the same time.[26,27,2] In Fig. 2 the same tendency can be observed inside the LCFS. In agreement with Ref. 2 the effect is more pronounced deeper in the plasma, whereas at the LCFS the Li-beam diagnostic does not observe a significant change.

In the SOL the effect is reversed, the relative fluctuation amplitudes increase with increasing average density. This result is in contrast to the observation on the Toroidal Experiment for Technically-Oriented Research (TEXTOR),[28] where the relative density fluctuation level just outside the limiter was seen to decrease. This reversed tendency in the SOL of W7-AS might be understood on the basis of the observation that the density scale length decreases with increasing average density. This behavior clearly showed up in more detailed investigations of the SOL density profile.[21] Assuming that the radial size of the turbulent structures stays constant, the relative density fluctuation amplitude should increase with decreasing scale length and thus with increasing average density (mixing length estimate). This reasoning involves that the density scale length is not determined by SOL turbulence, and anomalous transport might be more closely related to wave-like fluctuations.

Characteristic changes in confinement time are observed on W7-AS as a function of ι_a and magnetic shear,[29] which are thought to be an effect of anomalous transport changes at the edge. A similar high sensitivity of the parameters of wave-like fluctuations to changes in magnetic confinement suggests that they might be connected to anomalous transport. However, fluctuation amplitudes for $r/a>0.8$ were not found to be significantly lower for good confinement discharges than for bad confinement ones in the case of high density $[n_e(\max)\approx 6\times 10^{19}\,\mathrm{m}^{-3}]$. Conversely, as was shown in Sec. III C, at low electron densities the wave-like fluctuations disappeared for a certain magnetic configuration without a significant change in plasma confinement. These observations indicate that the rms amplitude of the wave-like fluctuations alone is in no case a good measure for anomalous transport at the edge.

ACKNOWLEDGMENTS

The work presented in this paper was supported by a contact between IPP-Garching and KFKI-RMKI. S.Z. would like to thank the W7-AS group for hospitality and constructive discussions during his stay in Garching.

[1] A. J. Wootton, B. A. Carreras, H. Matsumoto, K. McGuire, W. A. Peebles, Ch. P. Ritz, P. W. Terry, and S. J. Zweben, Phys. Fluids B **2**, 2879 (1990).
[2] U. Stroth, Plasma Phys. Controlled Fusion **40**, 9 (1998).
[3] S. J. Zweben and R. W. Gould, Nucl. Fusion **A25**, 171 (1985).
[4] M. Endler, H. Niedermeyer, L. Giannone, E. Holzhauer, A. Rudyj, N. Theimer, N. Tsois, and the ASDEX Team, Nucl. Fusion **35**, 1307 (1995).
[5] M. Endler, L. Giannone, K. McCormick, H. Niedermeyer, A. Rudyj, G. Theimer, N. Tsois, and S. Zoletnik, Phys. Scr. **51**, 610 (1995).
[6] J. W. Heard, T. P. Crowley, P. M. Schoch, R. L. Hickok, D. W. Ross, and B. Z. Zhang, Phys. Plasmas **2**, 3360 (1995).
[7] G. R. Hanson, J. H. Harris, J. B. Wilgen, C. E. Thomas, S. C. Aceto, L. R. Baylor, J. D. Bell, B. Brañas, J. L. Dunlap, A. C. England, C. Hidalgo, M. Murakami, D. A. Rasmussen, J. Sanches Sanz, J. G. Schwelberger, T. Uckan, and J. J. Zielinski, Nucl. Fusion **32**, 1593 (1992).
[8] R. J. Fonck, G. Cosby, R. D. Durst, S. F. Paul, N. Bretz, S. Scott, E. Synakowski, and G. Taylor, Phys. Rev. Lett. **70**, 3736 (1993).
[9] S. Sattler, H. J. Hartfuss, and W7-AS Team, Phys. Rev. Lett. **72**, 653 (1994).
[10] D. L. Brower, W. A. Peebles, and N. C. Luhmann, Jr., Phys. Rev. Lett. **55**, 2579 (1985).
[11] C. Hidalgo, J. H. Harris, T. Uckan, J. D. Bell, B. A. Carreras, J. L. Dunlap, G. R. Dyer, C. P. Ritz, A. J. Wootton, M. A. Meier, T. L. Rhodes, and K. Carter, Nucl. Fusion **31**, 1471 (1991).
[12] C. Hidalgo, J. H. Harris, T. Uckan, G. R. Hanson, J. D. Bell, M. A. Meier, C. P. Ritz, and A. J. Wootton, Nucl. Fusion **33**, 146 (1993).
[13] G. K. McCormick, S. Fiedler, G. Kocsis, J. Schweinzer, and S. Zoletnik, Fusion Eng. Des. **34-35**, 125 (1996).
[14] H. Renner, the W7-AS Team, NBI Group, ICF Group, and ECRH Group, Plasma Phys. Controlled Fusion **31**, 1579 (1989).
[15] S. Zoletnik, S. Fiedler, G. Kocsis, G. K. McCormick, J. Schweinzer, and H. P. Winter, Plasma Phys. Controlled Fusion **40**, 1399 (1998).
[16] J. Schweinzer, E. Wolfrum, F. Aumayr, M. Pöckl, H. Winter, R. P. Schorn, E. Hintz, and A. Unterreiter, Plasma Phys. Controlled Fusion **34**, 1173 (1992).
[17] M. Anton, T. Klinger, M. Häse, S. Zoletnik, J. Geiger, C. Görner, H. J. Hartfuss, R. Jaenicke, A. Weller, the W7-AS Team, NBI Group, and ECRH Group, J. Plasma Fusion Res. **1**, 259 (1998).
[18] J. Bleuel, G. Theimer, M. Endler, L. Giannone, H. Niedermeyer, the ASDEX and W7-AS Teams, in the *23rd EPS Conference on Controlled Fusion and Plasma Physics, Kiev, 1996* (European Physical Society, Petit-Lancy, 1997), Europhys. Conf. Abstracts, Vol. 20C, p. 727.

[19]L. Giannone, R. Balbin, H. Niedermeyer, M. Endler, G. Herre, C. Hidalgo, A. Rudij, G. Theimer, Ph. Verplanke, and the W7-AS Team, Phys. Plasmas **1**, 3614 (1994).
[20]V. Erckmann, F. Wagner, J. Baldzuhn, R. Brakel, R. Burhenn, U. Gasparino, P. Grigull, H. J. Hartfuss, J. V. Hoffman, R. Jaenicke, H. Niedermeyer, W. Ohlendorf, A. Rudij, A. Weller, S. D. Bogdanov, B. Bomba, A. A. Borschegovsky, G. Cattanei, A. Dodhy, D. Dorst, A. Elsner, M. Endler, T. Geist, L. Giannone, H. Hacker, O. Heinrich, G. Herre, D. Hildebrandt, V. I. Hiznyak, V. I. Il'in, W. Kasparek, F. Karger, M. Kick, S. Kubo, A. F. Kuftin, V. I. Kurbatov, A. Lazaros, S. A. Malygin, V. A. Malygin, K. McCormick, G. A. Müller, V. B. Orlov, P. Pech, H. Ringler, I. N. Roi, F. Sardei, S. Sattler, F. Schneider, U. Schneider, P. G. Schüller, G. Siller, U. Stroth, M. Tutter, E. Unger, H. Wolff, E. Würsching, and S. Zöpfel, Phys. Rev. Lett. **70**, 2086 (1993).
[21]G. Kocsis, S. Zoletnik, S. Fiedler, P. Grigull, G. Herre, K. McCormick, J. Schweinzer, and the W7–AS Team, in the *22nd EPS Conference on Controlled Fusion and Plasma Physics, Bournemouth, 1995* (European Physical Society, Petit-Lancy, 1996), Europhys. Conf. Abstracts, Vol. 19C, p. 269.
[22]M. Hirsch, P. Amadeo, M. Anton, J. Baldzuhn, R. Brakel, J. Bleuel, S. Fiedler, T. Geist, P. Grigull, J. J. Hartfuss, E. Holzhauer, R. Jaenicke, M. Kick, J. Kisslinger, J. Koponen, F. Wagner, A. Weller, H. Wobig, S. Zoletnik, and the W7-AS Team, Plasma Phys. Controlled Fusion **40**, 631 (1998).
[23]C. Görner, M. Anton, J. Geiger, W. von der Linden, A. Weller, S. Zoletnik, in the *24th EPS Conference on Controlled Fusion and Plasma Physics, Berchtesgaden, 1997* (European Physical Society, Petit-Lancy, 1998), Europhys. Conf. Abstracts, Vol. 21A, p. 1625.
[24]Y. J. Kim, K. W. Gentle, C. P. Ritz, T. L. Rhodes, and R. D. Bengtson, Nucl. Fusion **29**, 99 (1989).
[25]G. Vayakis, Nucl. Fusion **33**, 547 (1993).
[26]S. J. Zweben and R. W. Gould, Nucl. Fusion **23**, 1625 (1983).
[27]X. Garbet, J. Payan, C. Laviron, P. Devynck, S. K. Saha, H. Capes, X. P. Chen, J. P. Coulon, C. Gil, G. R. Harris, T. Hutter, A.-L. Pecquet, A. Truc, P. Hennequin, F. Gervais, and A. Quéméneur, Nucl. Fusion **32**, 2147 (1992).
[28]A. Komori, O. Mitarai, K. Yamagiwa, C. Honda, K. Kadota, J. Fujita, Y. T. Lie, U. Samm, A. Pospieszczyk, K. Hötkher, P. Bogen, and E. Hintz, Nucl. Fusion **28**, 1460 (1988).
[29]R. Brakel, M. Anton, J. Baldzuhn, R. Burhenn, V. Erckmann, S. Fiedler, J. Geiger, H. J. Hartfuss, O. Heinrich, M. Hirsch, R. Jaenicke, M. Kick, G. Kühner, H. Maaßberg, U. Stroth, F. Wagner, A. Weller, the W7-AS Team, ECRH Group, and NBI-Group, Plasma Phys. Controlled Fusion **39**, B273 (1997).